Hydrogen Adsorption on sp^2-Bonded Carbon Structures: Ab-initio Study

Young-Kyun Kwon*

Department of Physics and Research Institute for Basic Sciences, Kyung Hee University, Seoul 130-701, Korea

Using *ab-initio* density functional theory, we investigate both molecular and atomic hydrogen adsorption properties for sp^2-bonded carbon materials, such as graphene, fullerenes, and nanotubes, and their modified structures. Weak molecular hydrogen binding depends on different binding sites and hydrogen orientations. The energy barrier of the drift motion of a hydrogen molecule on the surface of graphitic materials is estimated to be small. We find that some modifications of the sp^2-bonding characters of graphitic materials, resulting from structural deformation or chemical doping, tend to enhance molecular hydrogen binding, and thus may increase the desorption temperature. Atomic hydrogen binds chemically or relatively strongly to the host carbon materials, resulting in a local modification of sp^2 carbon to sp^3 carbon. However, such strong atomic bonds easily breaks in the presence of unbound atomic hydrogen to form more favorable molecular hydrogen.

I. INTRODUCTION

Hydrogen storage is a key unsolved problem for producing fuel cells for hydrogen-powered automobiles or portable energy devices [1]. Several different techniques have been developed to tackle this problem. Among them are storage in tanks under high pressure [2,3], liquefying hydrogen at temperatures below 20 K with an energetically expensive cooling system [3,4], and forming metal or chemical hydrides [1, 3, 5]. These techniques, however, pose problems for practical use in automobiles: low hydrogen storage capacity, consumption of a great amount of energy to store or release hydrogen, limited number of cycling, and so on [1,3,5].

Since the first measurement of hydrogen uptake on carbon nanotubes [6], a number of research groups have focused their research on the use of carbon nanostructured materials, including nanotubes, as hydrogen storage materials due to their light weight and large surface area. There have been several optimistic reports [7–9] claiming that at ambient conditions, hydrogen can be stored in carbon nanostructured materials well beyond 6% by weight, which used to be the year 2010 target, but now is the 2015 (or beyond) target, set by the US Department of Energy for vehicular use. However, these measurements have not been reproduced by other research groups, or even within the same group. Moreover, it later was reported that an appreciable amount of hydrogen could be stored only at $T \lesssim 80$ K under an ambient

pressure up to 20 atm in carbon materials [10]. Other research groups have re-investigated the studies reported previously and have concluded that carbon materials, including nanotubes, store little hydrogen at ambient conditions, unlike previous measurements [1,11–13].

Here, we present the results of our theoretical investigation of hydrogen adsorption properties on sp^2-bonded graphitic carbon structures. This study would be a starting point to develop hydrogen storage materials that store and release hydrogen at temperatures near room temperature. To explore possible ways to improve the storage conditions, we have performed various first-principles calculations of both molecular and atomic hydrogen adsorption on sp^2-bonded carbon structures, such as graphite, nanotubes, and fullerenes. We have also studied the effects of structural modifications on hydrogen adsorption properties. We have already demonstrated that hydrogen binding energies on boron-nitride nanotubes [14], boron oxides [15, 16], and ethylene oxides [17] are indeed stronger than those on pure carbon materials as discussed below.

We find that the binding energies of H$_2$ on pure sp^2-bonded carbon materials range from $E_b \approx 55$ to 80 meV, depending on the structure, the adsorption sites and hydrogen orientation. This small binding energy is due to the very strong intramolecular H-H bond and its extremely small induced dipole moment, as well as to the chemically inert nature of the sp^2 system. The small binding energy leads to a desorption temperature as low as that of the liquid nitrogen at around atmospheric pressure, as estimated from the Langmuir gas adsorption the-

Table 1. Comparison of hydrogen binding energies and distances calculated with different basis sets and XC functionals for various configurations (different binding sites and hydrogen orientations). For configurations, see Fig. 1(a).

Methods	Binding energy [eV]	Binding distance [Å]
LDA + DZ	$0.08 \sim 0.10$	$2.7 \sim 2.8$
GGA + DZ	$0.00 \sim 0.02$	$3.0 \sim 3.1$
GGA + DZP	$0.05 \sim 0.07$	$3.0 \sim 3.1$

ory [18]. Our further studies reveal that the binding energy can be enhanced by modifying the sp^2-bonding character of the host materials. This can be done, for example, by generating structural defects or by chemical doping.

The remainder of the paper is organized as follows: In Sec. II., the computational methods used in the present study are briefly described. The effects of different exchange-correlation functionals and of different basis sets on the calculations are discussed and compared with experimental measurements available. Our calculated results for molecular hydrogen adsorption are presented in Sec. III. 1. for perfect 2D graphite or graphene, and in Sec. III. 2. for fullerenes and nanotubes. In Sec. III. 3., modified sp^2-bonded carbon structures, such as those containing a pentagon-heptagon pair defect, vacancy, and substitutional doping, are studied as possible pathways to improve hydrogen adsorption. Finally, we describe atomic hydrogen adsorption on sp^2-bonded structures in Sec. III. 4. Carbon atoms form relatively strong bonds with single hydrogen atoms, having a local sp^3-bonding character. Through molecular dynamics simulations, we investigate the stability of C-H bonds in the presence of free atomic hydrogen.

II. COMPUTATIONAL METHODOLOGY

To investigate the adsorption properties of hydrogen on graphitic carbon materials, we have carried out first-principles total energy calculations. The *ab-initio* pseudopotential density functional theory (DFT) [19], based on a linear combination of atomic orbitals basis [20,21], has been used. Since molecular hydrogen adsorbs on sp^2-bonded carbon materials by physisorption, we have performed calculations with various atomic basis sets, such as double-ζ (DZ) and double-ζ polarization (DZP), in combination with different exchange-correlation (XC) functionals – the local density approximation (LDA) and the generalized gradient approximation (GGA) [22].

As shown in Table 1, calculated hydrogen binding energies and distances are very sensitive to the choice of an XC functional and an atomic orbitals basis set. Comparing with various experimental measurements [10] and theoretical calculations [23] of molecular hydrogen binding energy on graphite or activated carbon, we find
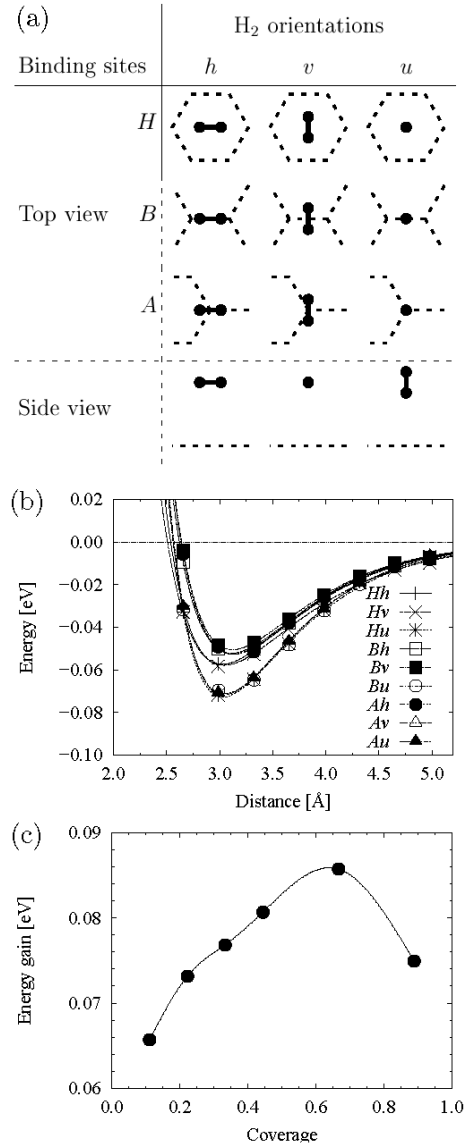

Fig. 1. (a) Schematic view of 9 different configurations formed by combining three binding sites — the center of a hexagon (H), a middle of a bond (B), and the top of a carbon atom (A) — and three H_2 orientations — horizontal (h), vertical (v), and upward (u). The dashed lines indicate underlying graphene structures and the hydrogen molecule is depicted by two solid circles with the solid line connecting the two. (b) Binding energies of a hydrogen molecule in a graphene sheet as a function of its distances from the graphene for 9 different configurations described in (a). (c) Energy gain per a H_2 molecule as a function of the number of adsorbed H_2 molecules. $N_{H_2} = 9$ means each hexagon is covered by a H_2 molecule.

that the LDA (GGA) with DZ overestimates (underestimates) the H_2 binding energy. A combination of the GGA and DZP gives the best agreement with the experimental measurements [10]. This trend has been shown in other systems, such as boron nitrides [14], boron oxides [15,16], and ethylene oxides [17]. Therefore, hereafter we

only present our results obtained using the GGA with DZP, unless otherwise stated.

We notice that there have been controversial arguments that the GGA or the LDA might not describe van der Waals (vdW) interactions due to their long-range nature. Several methodologies have been developed recently to describe such long-range interactions within DFT [24–27]. However, at this point, none have been accepted as reliable. While some *ad hoc* approaches [28–30] have been developed to produce potentials for describing the physisorption, we anticipate reliable exchange-correlation functionals to be developed within DFT that describe vdW interactions correctly. Here, we stress that our conventional DFT method with GGA cannot predict the hydrogen physisorption energy with an *extreme accuracy*, but is still valid to give comparisons between different structures and material, and to guide the search for better hydrogen storage materials, as described above. Hence, the results in this study can be understood as a reference within a given frame of computational methods.

We have used a norm-conserving nonlocal pseudopotential [31,32] and an atomic orbital basis [21] with an energy cutoff of 60 Rydbergs for the expansion of the wavefunctions. For the confinement energy shift, we have used 0.01 Ry, which defines the cutoff radii of the atomic orbitals. Each energy point consisting of a binding curve [*e.g.*, one in Fig. 1(b)] has been computed after carrying out geometrical relaxation in such a way that all the atoms were fully relaxed, but the center of mass of each species was fixed in order to maintain the given distance. The H_2 orientation also remained unchanged during the relaxation. After we had obtained several energy points, we fitted those data points to a Morse function with a form of

$$E(d) = E_B \left[1 - \left(1 - e^{-\alpha(d-d_B)} \right)^2 \right] + E_\infty , \quad (1)$$

where E_B, d_B, α, and E_∞ are fitting parameters. E_B corresponds to the binding energy at d_B, which is the equilibrium binding distance. Near d_B, this equation can be approximated by a harmonic function, $E(d) \approx -E_B \left[1 - \alpha^2 (d - d_B)^2 \right] + E_\infty$, from which the force constant is determined by using the third parameter α to be $k = 2E_B\alpha^2$. The fourth one, of course, is a constant shift to set the reference at infinity. For bound systems, the first and the third parameters should satisfy $E_B < 0$ and $\alpha > 0$.

We performed our calculations using various sizes of the unit cell to examine the finite size effects of supercells. For graphene, we found that a 4×4 supercell containing 32 carbon atoms was sufficiently large to ignore the effect of a hydrogen located at a neighboring cell. Moreover, we set the interlayer distance to be $d \approx 30$ Å along the c-axis to prevent neighboring sheets from influencing the hydrogen binding property. To emulate isolated C_{60} fullerenes, we used a face-centered cubic lattice structure, which is a known structure of solid C_{60},

with a lattice constant of $a \approx 40$ Å. For nanotubes, we chose $(5,5)$ and $(10,10)$ armchair nanotubes with 3 unit-cells along the tube axis. Along the perpendicular direction, triangular lattices were used with lattice constants $a \approx 37$ Å and $a \approx 60$ Å for $(5,5)$ and $(10,10)$ nanotubes, respectively.

III. RESULTS AND DISCUSSION

1. Hydrogen Adsorption on Perfect Graphene

First, we calculated the binding energy of molecular hydrogen on a graphene surface for nine different configurations, as summarized in Fig. 1(a). These configurations are obtained from a combination of three binding sites of the graphene — the center of a hexagon (H), the top of a carbon atom (A), and the middle of a bond (B) — and three different orientations of a hydrogen molecule — horizontal (h), vertical (v), and upright (u) orientations. Figure 1(b) shows the energies as a function of distances between the hydrogen molecule and the graphene surface for the nine configurations. The nine configurations are categorized into three groups in accordance with the magnitudes of the binding energies, as displayed in Fig. 1(b). The binding energy of the first group, comprised of three configurations (Hu, Au, and Bu), is calculated to be $E_B \approx 72$ meV, whereas those of the second group, consisting of Hh, and Hv configurations, and the other group, composed of the rest of the configurations (Ah, Av, Bh, and Bv), are calculated to be $E_B \approx 58$ meV, and $E_b \approx 53$ meV, respectively. It is found that the upright orientation of a H_2 molecule gives the largest binding energy, regardless of binding sites; and for a given hydrogen orientation, the H_2 binding is relatively stronger at the hexagonal center (H) than at other sites (A and B). Our calculated binding energy is in very good agreement with experiments [33–35].

From the energy difference between different configurations, we can estimate the maximum corrugation of the energy surface for hydrogen on the graphene surface to be $\Delta E_{\max} \approx 20$ meV. However, by keeping an orientation upright (u) position, for which the energy barrier for H_2 drift is only $\lesssim 1$ meV, hydrogen may drift over the graphene surface rather than stay on one binding site, even at a low temperature. Indeed, we observed that hydrogen molecules were floating around on a graphene surface and on a nanotube, even at 20 K, through our first-principle molecular dynamics simulations [36].

The equilibrium binding distance, at which the binding energy is minimum, is in the range of $d_B \approx 3.0 \sim 3.1$ Å, as shown in Fig. 1(b). This result leads to the very significant conclusion that the hydrogen molecules are not likely to be stored in-between graphite layers, which are ~3.4 Å apart from each other, nor in-between tube walls in multiwall nanotubes unless inserted under very high pressure. Hydrogen may,

however, be stored in the interstitial channels in a rope consisting of (10,10) nanotubes or those with a similar diameter, where the distance between the center of an interstitial channel and a tube wall is ~3.0 Å, which is about the equilibrium binding distance. Using the Mulliken population analysis, we calculated the charge transfer between the H_2 molecule and the graphene sheet. At the equilibrium binding distance, the computed charge transfer is $\Delta q \lesssim 0.02e$, regardless of configurations.

The binding energy is related to a characteristic temperature, T_d, called the desorption temperature, at which the adsorbates evaporate from the host materials. To estimate the desorption temperature at a given pressure, we used the van't Hoff equaiton and the Langmuir's gas adsorption theory [37]. For this estimate, several assumptions were made: multiple-layer adsorption is not allowed; interactions between hydrogen molecules are not considered, that is, each H_2 molecule has the same heat of adsorption, independent of coverage; the entropy of adsorbed hydrogen is very similar to that of liquid hydrogen [38]; and each hexagon of graphite can possess, at most, one hydrogen molecule at a maximum coverage. Coverage is defined as $\Theta = 2N/N_C$, where N is the number of adsorbates or H_2 molecules, and N_C is that of carbon atoms in a unit cell. The estimated desorption temperature is in the range of $T_d \approx 60 - 80$ K at around one atmospheric pressure, which is significantly lower than room temperature. This then leads to the necessity of significant cooling of the material for hydrogen storage purposes.

This rather simple estimate was reinvestigated by using a microscopic study based on DFT. To study the dependence of the binding energy on coverage, we performed a full geometry optimization every time an additional H_2 molecule was added to the host material [39]; then, the energy gain per adsorbate, E_g, defined by

$$E_g = (E_{B,N} - NE_{B,1})/N , \qquad (2)$$

was calculated. Here, $E_{B,N}$ is the total binding energy when N hydrogen molecules are adsorbed, and E_g is given with respect to $E_{B,1}$, with high E_g values corresponding to large gain in binding energy. The initial configuration was Hu. As displayed in Fig. 1(c), the energy gain increases as hydrogen molecules are added until the coverage becomes $\Theta \approx 0.6$, where adsorbed H_2 molecules form the most ordered structure. The increase in the energy gain is attributed mainly to dipole-dipole interactions between H_2 molecules. As more H_2 molecules are added, they become too close to each other, and the energy gain is reduced.

2. Hydrogen Adsorption on Fullerenes and Nanotubes

Similar studies were performed on fullerenes and carbon nanotubes to investigate the effects of curvature on
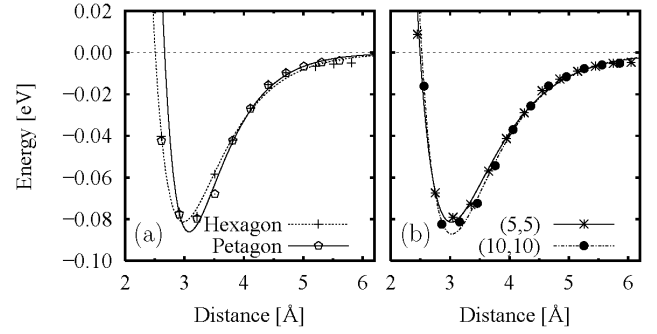

Fig. 2. Binding energies of the hydrogen molecule as a function of its distances from the outside surfaces of C_{60} (dashed line with open triangles), $(5,5)$ (solid line with stars) and $(10,10)$ (dash-dotted line with solid circles) nanotubes. Only a configuration Hu is considered in all cases.

the binding properties of hydrogen. For those structures, there are apparently two geometrically different sides for adsorption, *i.e.*, the inner and outer sides of the structures. These two sides may exhibit different adsorption energies due to the curvature. First, we consider the binding characters on the outer sides.

Figure 2 shows the calculated binding energy curves for the configuration of Hu as a function of H_2 distances from the surfaces of three selected structures of a C_{60} molecule (Fig. 2(a)), a $(5,5)$ nanotube and a $(10,10)$ nanotube (Fig. 2(b)) with the hydrogen molecule being adsorbed on the outer surface of each system [40]. Note that here we only show the binding energy curves for the Hu configuration because the trends of the binding energies for different configurations are similar to those described in Sec. III. 1. for graphene. Overall, the binding energies of fullerenes and nanotubes are larger by ~20 meV than those computed on graphene.

C_{60} contains not only hexagons, but also twelve pentagons. We compared the binding energy on top of a hexagon center with that on top of a pentagon center for the u orientation. As shown in Fig. 2(a), the binding energy on the pentagon is a little stronger than on the hexagon, but the difference appears to be small.

The effect of the curvature was studied with (5,5) and (10,10) nanotubes, and the calculated binding energies on both tubes were about $10 \sim 20$ meV stronger than on graphene due to the curvature, but the difference between the two tubes appears not to be significant, as shown in Fig. 2(b).

Although it would be practically very difficult to put hydrogen molecules inside the fullerenes, it would be instructive to estimate the hydrogen binding energy on the inner surface of C_{60}, as well as on those of nanotubes. Actually, hydrogen molecules were successfully inserted into C_{60} recently [41–43]. Unlike on outer surfaces, it is impossible to plot the entire binding energy curves. Instead, we estimated the binding energy from the total energy difference

$$E_B = E(C_{60} + H_2) - E(C_{60}) - E(H_2),$$

where the first two terms on the right-hand side are the total energies of the C_{60} and H_2, respectively, and $E(C_{60} + H_2)$ is that of the H_2-encapsulated C_{60}. We would like to point out one issue considered carefully in such calculations. Our *ab-initio* calculations are based on a linear combination of atomic orbitals. In order to estimate reliable values of the binding energy and the distance, we kept the total number of atomic orbitals bases to be the same while calculating the total energies for all cases. For example, we calculated the total energy of H_2 in the presence of 60 ghost carbon atoms for consistency. Its validity was confirmed by applying the same scheme outside the C_{60}.

The binding energy is found to be enhanced on the inner surface of the C_{60} because more carbon atoms contribute to the interaction with the hydrogen due to the curvature. The same trends were found inside the $(5,5)$ nanotube. The calculated binding energies are $E_B \approx 0.21$ and 0.18 eV on the inner surfaces of the C_{60} and the $(5,5)$ nanotube, respectively. The effect of hydrogen orientation on the binding is negligible. The diameters of the C_{60} and the $(5,5)$ nanotube are approximately $d \approx 6.7 \sim 6.9$ Å, which is about twice the hydrogen binding distance; thus their inner surfaces provide stronger binding sites than their outer counterparts because the vdW type interaction or physisorption is usually proportional to the size of the contact surface area. On the other hand, inside the $(10,10)$ nanotube, whose diameter is about 13.5 Å, the binding energy is about 0.1 eV, showing much smaller enhancement, because the "effective" contact area is not significantly larger than its outside surface or the flat graphene surface. The effective storage capacity on the inner surface is, however, apparently much smaller than that on the outer sides due to the limited space.

3.   Hydrogen Adsorption on Modified sp^2-bonded Structures

The binding of hydrogen on sp^2-bonded systems occurs through rather weak interactions that mainly originate from induced dipole-dipole interactions. Other mechanisms, such as weak hybridization of orbitals and higher-moment interactions, also contribute to the binding. The induced dipole moment is, however, very small because the intramolecular H–H bond is quite rigid, and the charge density of the sp^2-bonded materials is rather uniform at the equilibrium hydrogen adsorption distance of about 3.0 Å. In order to enhance the binding of molecular hydrogen to the substrate, it is necessary to change its reactivity, which may be achieved by disturbing the charge distribution or changing the local electronic structure. As direct and efficient ways to accomplish this goal,

we consider various modifications on sp^2-bonded carbon materials, including (i) introduction of defect structures such as pentagons, heptagons, pentagon-heptagon pairs, or vacancies, (ii) implantation of impurities, and (iii) intercalation of impurities, all of which will induce deviations from the regular sp^2-bonding.

Theory and experiment have shown that these modified configurations are more reactive than the perfect hexagonal structures [5,44]. The admixture of sp^2 bonding with sp^3 bonding in these defect structures could introduce partially unsaturated bonds, which may enhance the chemical reactivity. In terms of electronic structures, such changes in bonding character lead to modifications of the electronic states near the Fermi level to which the binding of gas molecules may be sensitive. The binding energy could, hence, be controlled through modifications of the sp^2-bonding. As illustrations of this general concept, we present here our results of the calculated binding energy of hydrogen on defective structures. Among them are the two examples displayed in Figs. 3(a) and 3(b).

A. Pentagon-heptagon defects

The first defective structure considered is two pairs of pentagon-heptagon on a graphene monolayer generated by rotating a bond of a hexagon ring by 90°, called the Stone-Wales transformation, as depicted in Fig. 3(a). Such pentagon-heptagon structures can be produced by mechanical deformations [45], such as stretching, bending, or twisting, or by electron irradiations [46]. Figure 3(c) shows the calculated binding energies on pentagon and heptagon sites are about 82 and 90 meV, respectively, which corresponds to an increase of about 20–30% from that of a perfect graphene sheet.

B. Vacancies

Next, we considered various structures with a carbon vacancy, which have recently been investigated using the high resolution TEM [47]. Figure 3(d) shows binding energy curves of hydrogen on a two-carbon-atom (dimer) vacancy for different H_2 orientations h, v, and u, which are the same as those defined in Fig. 1(a). In this case, there are four unpaired dangling bonds generated by removing two carbon atoms. We did not saturate those dangling bonds with hydrogen atoms because they are quite close to each other, so saturation is energetically unfavorable. Therefore, one might expect that the h orientation would give a larger binding energy than other orientations because H_2 in this orientation could be placed similarly as the removed carbon dimer. However, its corresponding binding energy is weaker than that in the u orientation, and is similar to that in the v orientation, as shown in Fig. 3(d). Compared to those
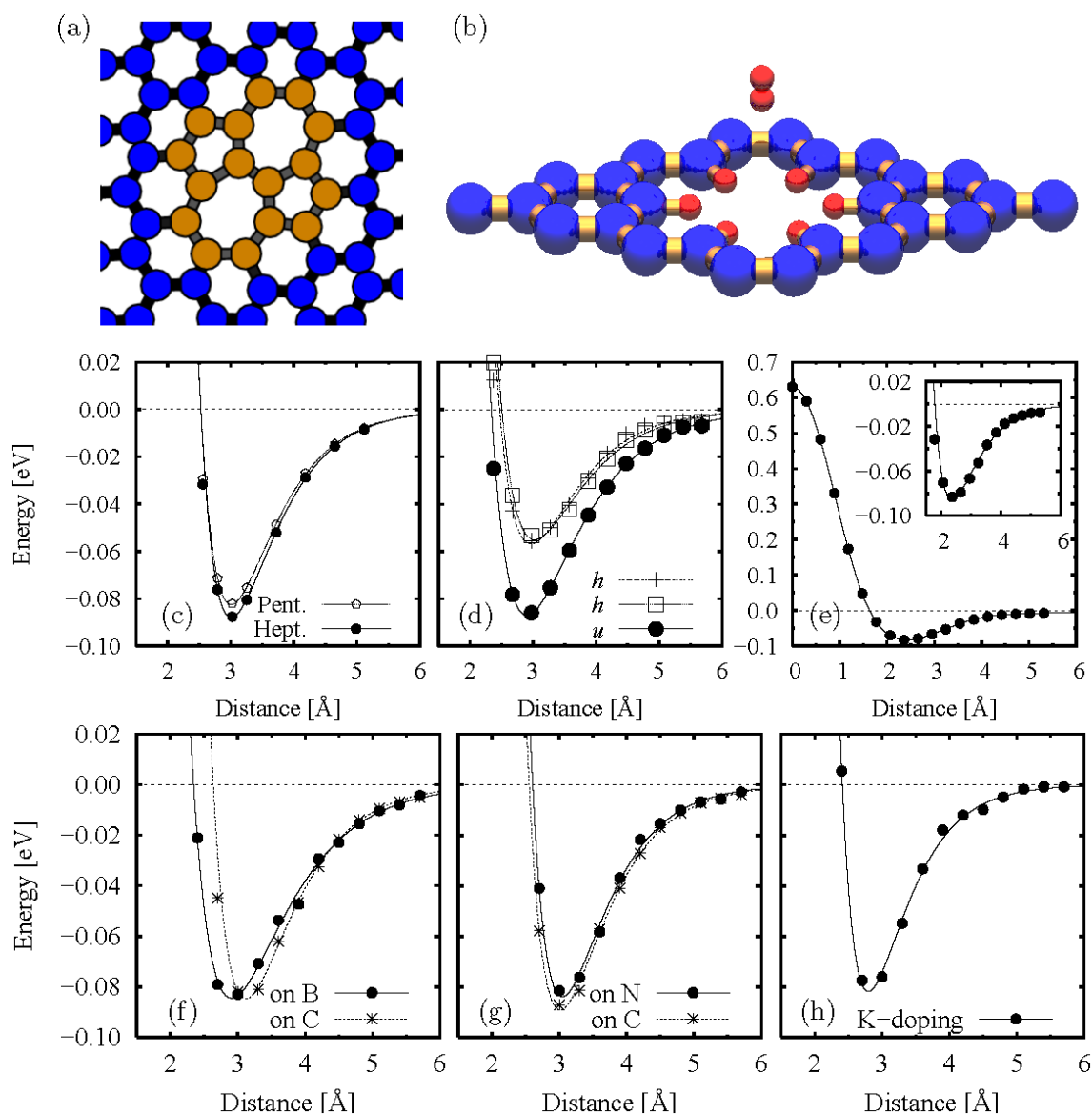
Fig. 3. (Color online) (a) 5-7 defect structure and (b) 6 carbon atom vacancy with 6 hydrogen atoms saturating carbon dangling bonds. Binding energies of the hydrogen molecule as a function of its distances from defected graphene structures on (c) 5-7 defect shown in (a), (d) two-atom vacancy (no hydrogen atom for saturation), (e) six-atom vacancy shown in (b), substitutional doping sites – 1 carbon atom out of 32 atoms in a supercell has been substituted either (f) by 1 boron (B) atom or (g) by 1 nitrogen (N) atom. (h) Binding energy of H_2 on graphene doped with 1 potassium (K) atom, which is just adsorbed on top of one carbon atom.

on perfect graphene, H_2 in the u orientation binds on this defect site more strongly by about 30%, but there is no binding enhancement in other orientations.

More carbon atoms were removed to see the effect of the sizes of vacancies on H_2 adsorption. The binding energies of H_2 for different vacant sites (up to 5-atom vacancy) were found to be similar to those displayed in Fig. 3(d). Once 6 carbon atoms in a hexagonal ring have been removed, then this type of vacancy becomes more stable by saturating each dangling bond with a hydrogen atom, unlike those smaller vacancies, as seen in Fig. 3(b). This saturation is expected to occur in real experimental

conditions. The binding energy itself is almost the same as those for other smaller vacancies, as shown in an inset of Fig. 3(e), although no unsaturated dangling bonds exist in this six-atom vacancy. The calculated binding energy of a u-oriented hydrogen molecule on top of the vacancy is found to be $E_b \approx 85$ meV. In addition, this vacant hole is large enough for one hydrogen molecule to go through with an energy barrier of only ≈ 0.63 eV, as shown in Fig. 3(e).

C. Substitutional doping

We calculated the molecular hydrogen binding energy on several systems where some of the host atoms were replaced by impurity atoms. The first system considered was a graphene sheet on which one boron atom was substituted for one carbon atom. For the particular case of 31 carbon atoms and one boron atom in a unit cell, which corresponds to about 3% boron-impurity concentration, the binding energy of molecular hydrogen was calculated to be about 90 meV on top of a boron atom, which is about 25% larger than that for a pure carbon graphene, as shown in Fig. 3(f). Sites right next to the impurity atom also exhibit binding enhancement, but those far from the impurity atom do not show any significant improvement. To investigate the dependence of hydrogen binding on the impurity concentration, we increased the boron-impurity concentration by further replacing carbon atoms by boron atoms and generated B_4C_{28} (boron concentration of 12.5%) and B_8C_{24} (25%) structures. As the concentration increased, the boron sites continued to exhibit stronger binding by 10 to 20%. Moreover, the hydrogen binding energy was also enhanced by a similar amount on other sites, such as on a nearest-neighbor C atom of the boron impurity, as shown in Fig. 3(f). Averaging over all sites, the increase in the binding energy is about 10 to 20% at the large boron-substitutional doping limit. Similar adsorption behaviors were observed on nitrogen-doped graphene, as shown in Fig. 3(g).

D. Additions

We also investigated the hydrogen binding on K-doped sp^2 graphitic carbon structures, including graphene, C_{60}. Unlike the substitutional doping discussed above, a potassium atom was just added to the system to form an intercalated system. Around the K atom, the H_2 binding was enhanced, and a typical binding curve is shown in Fig. 3(h). Similar to the other modified carbon structures as seen above, the binding enhancement is about 10–20%.

4. Atomic Hydrogen Adsorption

We also calculated the binding energies of atomic hydrogen adsorbed on sp^2-bonded carbon materials. As we did for molecular hydrogen adsorption, we considered three different binding sites, H, B, and A; the notation is the same as that used in Fig. 1(a). Note that there is no hydrogen orientation to be considered. For the first two binding sites, the calculated binding energy curves are shown in Fig. 4(a). The binding energy ($\sim$0.27 eV) on the H site, or on the center of a hexagon, is much weaker than that ($\sim$0.35 eV) on the B site. Moreover,
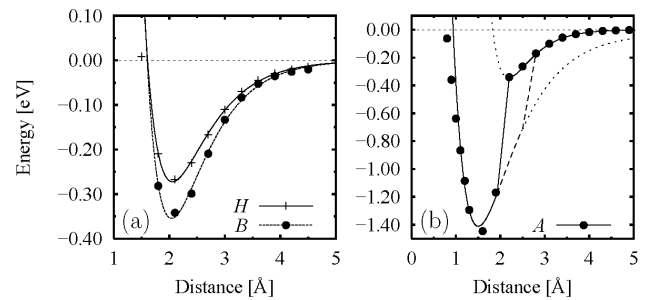

Fig. 4. Atomic hydrogen binding energies as a function of its distances from graphene surface, on top of (a) H, B, and (b) A binding sites. (See Fig. 1(a) for binding site indices.) It is shown that an abrupt transition from "intermediate" bond to chemical bond occurs near $d \approx 2$ Å when the hydrogen atom approaches to graphene, but the reverse transition occurs at larger distance when it moves away from graphene, displayed with dashed line.

both are still much smaller than a typical energy scale for the chemical bonding, but larger than that for physical adsorption. The binding distances in both cases are $d \approx 2$ Å, which is long in a chemical sense, but relatively short in a vdW sense. Such an "intermediate" bonding character is assigned to a combination of the inert nature of sp^2-bonded graphitic structures and the reactiveness of atomic hydrogen.

For the A site, the binding energy curve appears quite interesting, as shown in Fig. 4(b). As the hydrogen atom approaches the graphene on top of a carbon atom, the binding curve shows an intermediate feature similar for an H or a B site until the distance between the H atom and the C atom becomes $d \approx 2.1$ Å. As soon as they are closer than that, the carbon atom, which was originally sp^2-bonded, forms a chemical bond with the hydrogen atom in addition to three neighboring carbon atoms, resulting in a local sp^3-bonded carbon. This "bond transition" from an *intermediate bond* to a *chemical bond* may occur spontaneously with little reaction barrier. This transition is clearly seen in Fig. 4(b) along the solid line. Subsquently, the binding energy is $E_B \sim 1.4$ eV at a binding distance of $d \approx 1.5$ Å. Note that the distance used in the curve is *not the C-H bond length*, but a distance between the hydrogen atom and the center of mass of the graphene in the unit cell including the sp^3-bonded carbon atom. We found that even though the distance varied from $d = 0.6$ Å to 2.0 Å in the curve, the actual C-H bond length was kept around $1.2 \sim 1.3$ Å. Moreover, we found that when adsorbed hydrogen atom moves away from the graphene, it follows a different path, exhibiting a hysteresis as shown in Fig. 4(b). This hysteresis may be attributed to the chemical nature of the bond.

There have been several computational studies on atomic hydrogen adsorption on sp^2-bonded carbon materials [48–52]. These calculations show a wide range ($0.1 \sim 2$ eV) of binding energy values, which can be explained by the range of our calculated binding ener-
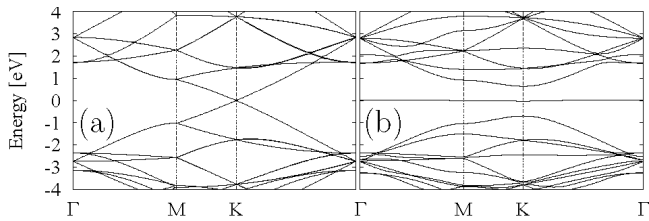
Fig. 5. Electronic bandstructures of (a) pristine graphene and (b) graphene adsorbing a hydrogen atom. Graphene contains 32 carbon atoms in its unit cell. The pristine graphene shows semi-metallic characteristics clearly crossing two bands at K point, whereas hydrogen-bonded graphene opens a gap with a band gap of ~1.3 eV due to a local sp^3 bonding and also shows a defect state, which essentially match with its Fermi level.

gies obtained for the different binding sites H, B, and A and by the different exchange-correlation functionals used. Recently, atomic hydrogen adsorption on graphitic structures has been observed [53].

We also computed the electronic band structure of the atomic-hydrogen-adsorbed graphene and compared it with that of the pristine graphene. Figure 5 displays the computed electronic bandstructures of the pristine graphene with 32 carbon atoms in a unit cell and the graphene with hydrogen atom adsorbed (1 hydrogen atom in graphene with 32 carbon atoms in a unit cell). For the latter case, its geometry was taken at the equilibrium point ($d \approx 2$ Å) in Fig. 4(b). The pristine graphene exhibits the semimetallic characteristics of crossing bands at the K point whereas the crossing bands repel each other to open a band gap of $E_g \approx 1.3$ eV due to a local transition from sp^2 carbon to sp^3, but with a defect state near the Fermi level due to the adsorbed hydrogen atom. It is noticeable that we observe a defect state due to the atomic hydrogen at $E \approx 0$ eV as well as two other nearly flat bands around $E \approx 2$ eV and $E \approx -2.5$ eV with respect to $E_F = 0.0$ eV.

We also checked the stability of the chemical bond between a hydrogen atom and a carbon atom in graphene in the presence of "free" hydrogen atoms. Through our molecular dynamics simulations, we found that when a free hydrogen atom passes near by the bound hydrogen atom, the latter H atom breaks the C-H bond easily and recombines with the former H atom to become a more stable H_2 molecule suggesting that although we could find an easy way to dissociate molecular hydrogen to produce atomic hydrogen, it is unlikely that atomic hydrogen can be stored in graphitic carbon structures in the presence of *free* atomic hydrogen.

IV. SUMMARY

In summary, using a first-principles density functional formalism, we investigated the adsorption properties of hydrogen on carbon materials. We found that hydrogen molecules weakly bind on sp^2-bonded carbon materials by a van der Waals type interaction, thus desorbing at temperature around the liquid nitrogen temperature. Curved graphitic carbon structures, such as fullerenes and nanotubes, exhibit higher hydrogen binding than their flat counterpart or graphene. We proposed that modifying sp^2-bonds by using , for example, structural defects, and chemical doping, enhances the binding energy by 5 – 20%.

Atomic hydrogen adsorption was also investigated on the graphene surface. We found that the calculated binding energy displays a wide range of values depending on the binding sites. We also found that a special configuration exhibits the binding curve showing a hysteresis in the transition between an intermediate bond and a chemical bond. However, when another free hydrogen atom exists nearby, the bound hydrogen atom can be easily detached to form a molecular hydrogen.

REFERENCES

[1] M. Dresselhaus *et. al.*, *Report of the Basic Energy Scieces Workshop on Hydrogen Production, Storage, and Use*, 2nd printing (May 13–15, 2003), and references therein. Available at http://www.sc.doe.gov/bes/hydrogen.pdf.

[2] R. K. Ahluwalia, T. Q. Huaa, J.-K. Peng, S. Lasher, K. McKenney, J. Sinha and M. Gardiner, Int. J. Hydrogen Energ. **35**, 4171 (2010).

[3] U. M. Nour, S. Awad, S. Yusup and S. Sufian, J. Appl. Sci. **10**, 1200 (2010).

[4] S. H. Ho and M. M. Rahman, J. Thermophys. Heat Tr. **24**, 374 (2010).

[5] L. Schlapbach and A. Züttel, Nature **414**, 353 (2001).

[6] A. C. Dillon, K. M. Jones, T. A. Bekkedahl, C. H. Kiang, D. S. Bethune and M. J. Heben, Nature **386**, 377 (1997).

[7] A. Chambers, C. Park, R. T. K. Baker and N. M. Rodriguez, J. Phys. Chem. B **102**, 4253 (1998).

[8] P. Chen, X. Wu, J. Lin and K. L. Tan, Science **285**, 91 (1999).

[9] C. Liu, Y. Y. Fan, M. Liu, H. T. Cong, H. M. Cheng and M. S. Dresselhaus, Science **286**, 1127 (1999).

[10] C. C. Ahn, Y. Ye, B. V. Ratnakumar, C. Witham, R. C. Bowman, Jr. and B. Fultz, Appl. Phys. Lett. **73** 3378 (1998).

[11] B. Panella, M. Hirscher and S. Roth, Carbon **43**, 2209 (2005).

[12] R. Ströbela, L. Jörissen, T. Schliermann, V. Trapp, W. Schütz, K. Bohmhammel, G. Wolf and J. Garche, J. Power Sources **84**, 221 (1999).

[13] W.-C. Xu, K. Takahashi, Y. Matsuo, Y. Hattori, M. Kumagai, S. Ishiyama, K. Kaneko and S. Iijima, Int. J. Hydrogen Energ. **32**, 2504 (2007).

[14] S.-H. Jhi and Y.-K. Kwon, Phys. Rev. B **69**, 245407 (2004).

[15] S.-H. Jhi, Y.-K. Kwon, K. Bradley and J.-C. P. Gabriel, Solid State Commun. **129**, 769 (2004).

[16] S.-H. Jhi and Y.-K. Kwon, Phys. Rev. B **71**, 035408 (2005).

[17] S. Woo and Y.-K. Kwon, Phys. Rev. B **79**, 075404 (2009).

[18] I. Langmuir, J. Am. Chem. Soc. **38**, 2221 (1916).

[19] M. L. Cohen, Phys. Scr. **T1**, 5 (1982).

[20] D. Sanchez-Portal, P. Ordejón, E. Artacho and J. M. Soler, Int. J. Quantum Chem. **65**, 453 (1997).

[21] P. Ordejón, Phys. Status Solidi B **217**, 335 (2000).

[22] J. P. Perdew, K. Burke and M. Ernzerhof, Phys. Rev. Lett. **77**, 3865 (1996).

[23] J. S. Arellano, L. M. Molina, A. Rubio and J. A. Alonso, J. Chem. Phys. **112**, 8114 (2000).

[24] Y. Andersson, D. C. Langreth and B. I. Lundqvist, Phys. Rev. Lett. **76**, 102 (1996).

[25] E. Hult, Y. Andersson, B. I. Lundqvist and D. C. Langreth, Phys. Rev. Lett. **77**, 2029 (1996).

[26] W. Kohn, Y. Meir and D. E. Makarov, Phys. Rev. Lett. **80**, 4153 (1998).

[27] H. Rydberg, M. Dion, N. Jacobson, E. Schröder, P. Hyldgaard, S. I. Simak, D. C. Langreth and B. I. Lundqvist, Phys. Rev. Lett. **91**, 126402 (2003).

[28] M. Kamiya, T. Tsuneda and K. Hirao, J. Chem. Phys. **117**, 6010 (2002).

[29] X. Wu, M. C. Vargas, S. Nayak, V. Lotrich and G. Scoles, J. Chem. Phys. **115**, 8748 (2001).

[30] T. V. Mourik and R. J. Gdanitz, J. Chem. Phys. **116**, 9620 (2002).

[31] N. Troullier and J. L. Martins, Phys. Rev. B **43**, 1993 (1991).

[32] L. Kleinman and D. M. Bylander, Phys. Rev. Lett. **48**, 1425 (1982).

[33] P. Bernard and R. Chahine, Langmuir **17**, 1950 (2001).

[34] H. Marsh, D. Crawford, T. M. O'Grady and A. Wennerberg, Carbon **20**, 419 (1982).

[35] C. M. Brown, T. Yildirim, D. A. Newmann, M. J. Heben, T. Gennett, A. C. Dillon, J. L. Alleman and J. E. Fischer, Chem. Phys. Lett. **329**, 311 (2000).

[36] Y.-K. Kwon, in preparation.

[37] The van't Hoff equation, describing the equilibrium pressure (p) of gas adsorption at temperature (T), is given as $\log p = -\Delta H/k_B T + \Delta S/R$, where ΔH is the heat of adsorption, k_B the Boltzmann constant, ΔS the change in entropy, and R the gas constant. The desorption temperature is defined as the temperature that gives an equilibrium pressure of 1 atm.

[38] *Handbook of Chemistry and Physics*, 81st ed., edited by D. R. Lide (CRC Press, New York, 2000).

[39] An H_2 molecule is added in such a way that the distance between adsorbates is kept as far as possible.

[40] J. S. Arellano, L. M. Molina, A. Rubio, M. J. López and J. A. Alonso, J. Chem. Phys. **117**, 2281 (2002).

[41] K. Komatsu, M. Murata and Y. Murata, Science **307**, 238 (2005).

[42] M. Murata, Y. Murata and K. Komatsu, J. Am. Chem. Soc. **128**, 8024 (2006).

[43] S. Riahi, P. Pourhossein, A. Zolfaghari, M. R. Ganjali and H. Z. Jooya, Fuller. Nanotub. Car. N. **17**, 159 (2009).

[44] P.-X. Hou, S.-T. Xu, Z. Ying, Q.-H. Yang, C. Liu and H.-M. Cheng, Carbon **41**, 2471 (2003).

[45] B. I. Yakobson, C. J. Brabec and J. Bernholc, Phys. Rev. Lett. **76**, 2511 (1996).

[46] V. H. Crespi, M. L. Cohen and A. Rubio, Phys. Rev. Lett. **79**, 2093 (1997)

[47] A. Hashimoto, K. Suenaga, A. Gloter, K. Urita and S. Iijima, Nature **430**, 870 (2004).

[48] L. Jeloaica and V. Sidis, Chem. Phys. Lett. **300**, 157 (1999).

[49] Y. Ferro, F. Marinelli and A. Allouche, J. Chem. Phys. **116**, 8124 (2002).

[50] Y. Miura, H. Kasai, W. A. Diño, H. Nakanishi and T. Sugimoto, J. Phys. Soc. Jpn. **72**, 995 (2003).

[51] L. Hornekær, Ž. Šljivančanin, W. Xu, R. Otero, E. Rauls, I. Stensgaard, E. Lægsgaard, B. Hammer and F. Besenbacher, Phys. Rev. Lett. **96**, 156104 (2006).

[52] F. H. Yang, A. J. Lachawiec, Jr. and R. T. Yang, J. Phys. Chem. B **110**, 6236 (2006).

[53] R. Balog, B. Jørgensen, L. Nilsson, M. Andersen, E. Rienks, M. Bianchi, M. Fanetti, E. Lægsgaard, A. Baraldi, S. Lizzit, Z. Sljivancanin, F. Besenbacher, B. Hammer, T. G. Pedersen, P. Hofmann and L. Hornekær, Nat. Mater. **9**, 315 (2010).